THE APPLICATION OF THE ENTHALPY METHOD TO MODELLING THE TRANSIENT RECOVERY OF P-I-N DIODES AND G.T.O. THYRISTORS

F. Berz, P.A. Gough, J.A.G. Slatter

Philips Research Laboratories, Redhill, Surrey, England.

SUMMARY

The Enthalpy method has previously been used to model solid/liquid systems which contain moving interfaces between phases (e.g. the Stefan problem). We have used this approach to model the one-dimensional transient behaviour of semiconductor devices which contain electron-hole plasma regions with moving boundaries adjacent to depletion layers. The method has been employed using a finite difference scheme, with Gauss-Seidel iterations, and in a circuit based implementation. The advantage of the method is in reduced computational effort.

Two particular cases have been considered: the n-base p-i-n diode in reverse ramp recovery and the GTO thyristor under gated switch-off conditions. In the case of the p-i-n diode, where the plasma often recedes from both junctions at some stage during recovery, it is shown that the shape of the recovery characteristic is appreciably affected by the values of the reverse supply voltage and the series inductance. For the GTO thyristor, where the plasma recedes from the central junction, we have studied the influence on power dissipation during turn-off of the parameters of the wide lightly doped base, and the device polarity.

1. INTRODUCTION

The switch-off characteristics of p-i-n diodes and GTO thyristors can be modelled by solving the equations of transport and conservation of charge and the Poisson equation. This comprehensive approach requires a complex program and leads to appreciable computing time.

As a simpler alternative, which we use here, one can employ a regional approach. Under this scheme the transient behaviour of each device is determined essentially by the

evolution of the carrier densities inside the wide lightly doped base of the device. One divides this base into a part filled with plasma, where there are equal numbers of electrons and holes in high injection and, in the later stages of switch-off, one or two additional regions adjacent to the junctions where only one type of carrier is present (the region next to the blocking junction has an appreciable space charge). The boundaries between the plasma and these regions move during turn-off and the carriers within the plasma decay due to recombination and to extraction by the current. (For more details see sections 2.1 and 3, Figs. 2a and 9).

The regional approach has already been used by several authors for modelling recovery in pin diodes. Benda and Spenke simplified the problem further by some a priori assumptions as to the spatial distribution of the carriers concentration within the plasma [1]. Other authors did take into account the equations governing the plasma concentration [2,3,4]. The determination of the moving plasma boundaries requires however numerous iterations, especially when two boundaries rather than one are involved.

In the present paper we use the Enthalpy Method [5] which is particularly suited to this situation. This method has been developed for heat problems connected with melting and freezing, where a moving boundary arises at the solid/liquid interface (e.g. Stefan type problems [6]). It has been extended to other applications, but to our knowledge we are describing its first applications to semiconductors.

We shall deal here with 2 specific problems

a) Ramp recovery of p-i-n diodes.
b) Gate turn-off of thyristors. (Because the processes of plasma variation and space charge layer development that occur in GTO turn-off are similar in many aspects to those occurring in p-i-n diode recovery, the description of the turn-off process will be considered in less detail.)

2. RAMP RECOVERY OF P-I-N DIODES

2.1 Qualitative Description

Ramp Recovery is considered here with the pin diode connected to the external circuit shown in Fig. 1. In forward bias a current I_F (>0) is flowing through the diode. During recovery the diode is connected with a reverse voltage V_R and an inductance L_c. A more complex circuit could have been used, but the set-up considered here will give the main features of the ramp recovery.

The current I(t) during recovery is as follows

$$\frac{dI}{dt} = -\frac{V_R}{L_c} + \frac{V_{DIODE}(t)}{L_c} \qquad (1)$$

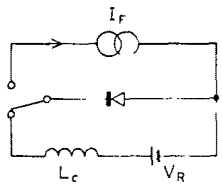

Fig 1

where t is the time, $V_{DIODE}(t)$ is the voltage developed in the diode. With the present sign conventions I is positive when it is in the same direction as I_F, V_R is positive, and $V_{DIODE}(t)$ is positive (except during the very first stages of recovery).

It is the evolution of V_{DIODE} with time which determines the transient current response I(t). At t=0 the carrier distribution corresponds to steady state. The recovery can be divided into 2 or 3 phases (see for example Fig. 2a,b).

In Phase 1 ($0<t<t_1$) the whole of the base, of width W, is occupied by the neutral plasma whose density decreases with time while remaining in high injection. During this phase $|V_{DIODE}(t)| << V_R$, and therefore, according to eq. (1)

$$\frac{dI}{dt} = -\frac{V_R}{L_c} \qquad (2)$$

In Phase 2 ($t_1 \leq t < t_2$), the neutral plasma moves away from the base/p^+ junction. It occupies the region $0<x<S(t)$. In the region $S(t)<x<W$ the only free carriers are holes which conduct the current.

In Phase 3 ($t>t_2$) the neutral plasma moves also away from the n^+/base junction. In the region $0<x<S^*(t)$ the only free carriers are electrons which carry the current. The neutral plasma lies between $S^*(t)$ and $S(t)$. Phase 3 does not necessarily arise, although it is often found during Ramp Recovery.

During Phases 2 and 3 most of the diode voltage V_{DIODE} develops in the regions between the plasma boundaries and the junctions ($S<x<W$, and $0<x<S^*$). As these regions widen V_{DIODE} becomes comparable to V_R. The variations of V_{DIODE} in time determine I(t) (see eq. (1) and Fig. 2b).

Fig. 2a.

$\frac{dI}{dt} = -100A/\mu s \quad V_R = 150V$

$I_F = 20A \quad Area = 0.1cm^2$

Diode parameters (see table I)

$W = 100\,\mu m$

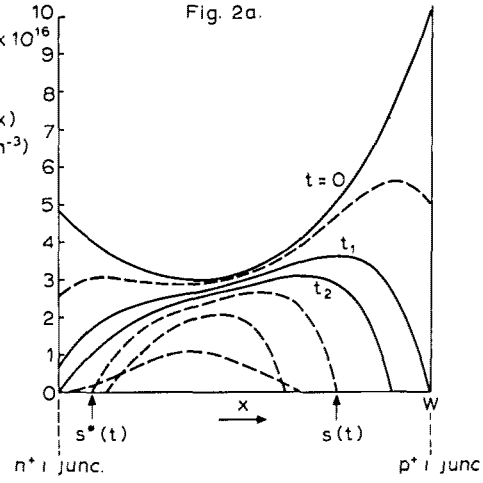

Fig 2b

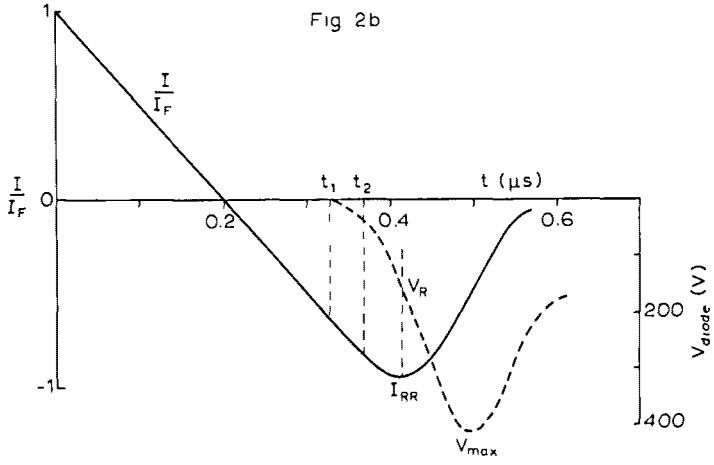

Analytical solutions have been obtained for the evolution of the plasma during Phase 1, for the case when recombination in the emitters and at the junctions can be neglected [7,8]. In the case where these recombinations are important one could still model Phase 1 by standard numerical methods such as were used already for step recovery [9].

Phases 2 and 3 where plasma boundaries are moving require however a modified approach. It is there that the Enthalpy method is of particular advantage.

2.2 Main Assumptions

The following assumptions are made:

*1. The problem is one-dimensional.
*2. The temperature of the diode is constant and uniform.
 3. The junctions are abrupt (as in epi-diodes).
 4. The base is n type.
 5. The doping N_D in the base is uniform.
 6. The lifetime τ in the base is constant.
*7. The plasma carrier density is much higher than N_D.
 8. The displacement current is neglected.

Assumptions 1, 2, and 7, marked here with stars, are essential. Assumptions 4, 5, 6 and 8 could be waived.

The present treatment could also be extended to take approximately into account the effect of diffused junctions (see [10]).

2.3 Fundamental Equations

A. In the Plasma Region. The derivation of equations (3) to (8ab) below is given in [11]. One has inside the plasma

$$\frac{\partial}{\partial x}\left[D_A(c)\,\frac{\partial c}{\partial x}\right] = \frac{\partial c}{\partial t} + \frac{c}{\tau} \tag{3}$$

where c is the carrier concentration. D_A is the ambipolar diffusion constant, which in general varies with c due to hole electron scattering ([12,13]).

The boundary conditions are as follows:

$$\text{At}\quad t = 0\quad c(x,0)\ \text{is given} \tag{4}$$

This is the carrier distribution in steady state in forward bias.

At the plasma boundaries (see Fig. 2a):

Two cases have to be distinguished during switch off:

1) When the plasma touches the junctions:

$$eD_A \left.\frac{\partial c}{\partial x}\right|_0 = -\frac{J}{1+b} + eh_n\, c^2(0,t) + es_n\, c(0,t) \tag{5a}$$

$$eD_A \left.\frac{\partial c}{\partial x}\right|_W = \frac{b\,J}{1+b} - eh_p\, c^2(W,t) - es_p\, c(W,t) \tag{5b}$$

J is the current density, taken here as positive when it flows from the p^+ to the n^+ emitter inside the diode i.e. from x=W to x=0 (this is contrary to usual conventions), e is the electronic charge, b the ratio of the electron/hole mobilities, h_n, s_n, h_p, s_p characterise the recombination in the n^+ and p^+ regions [14].

2) When the plasma is detached from the junctions one takes:

$$c(S^*,t) = K|J| \tag{6a}$$

$$c(S,t) = K|J| \tag{6b}$$

where one has in cgs practical units [11]

$$K = 1.04.10^{20}/N_d^{\frac{1}{2}} \tag{7}$$

and

$$eD_A \left.\frac{\partial c}{\partial x}\right|_{S^*} = \frac{-J}{1+b} - e|K| \frac{dS^*}{dt} \tag{8a}$$

$$eD_A \left.\frac{\partial c}{\partial x}\right|_{S} = \frac{bJ}{1+b} - e|K| \frac{dS}{dt} \tag{8b}$$

In Phase 1 one uses equations (5ab), in Phase 2 equations (5a)(6b) and (8b), and in Phase 3 equations (6ab) and (8ab).

B. Voltage drop across the diode

As was briefly described in section 2.1, the voltage drop across the diode determines the change of current I with time. The relation between V_{DIODE} and I is given by eq. (1).

The voltage drop V_{DIODE} can be written as

$$V_{DIODE} = V_{PJ} + V_S + V_{S*} \tag{9}$$

V_{PJ} is the voltage drop across the plasma ($S^*<x<S$), and the junctions. V_S and V_{S*} are the voltages developed in the regions $S<x<W$ and $0<x<S^*$, which appear during phases 2 and 3.

The voltage V_{PJ} which is given by well known equations [15], is usually much smaller than V_R. Its effect on dI/dt as given in eq. (1) is therefore very minor.

The major contribution to V_{DIODE} in eq. (1) is V_S in Phase 2 and $V_S + V_{S*}$ in Phase 3 (with $V_S >> V_{S*}$).

In deriving V_S and V_{S*} we have followed an approach similar to [1], while also taking into account the variation of the carrier mobilities with field, due to heating.

Let us briefly consider the derivation of V_S. The current in the region $S<x<W$ between the plasma and the p^+ junction is taken to be carried entirely by holes. This neglects the displacement current (cf assumption 8 of section 2.2) and any generation current which may arise in this region devoid of electrons. Moreover it is assumed that the current is entirely by drift. One therefore has

$$|J| = |J_p| = e\mu_p(E)\, p(x)\, E(x) \tag{10}$$

where J_p is the hole current density, $p(x)$ the hole density and $E(x)$ is the electric field (>0), $\mu_p(E)$ is the hole mobility, which is taken as

$$\mu_p = \frac{\mu_p^o}{1 + (\mu_p^o/v_{pl})E} \tag{11}$$

where $\mu_p{}^o$ is the hole mobility in low field and v_{pl} is the limiting hole velocity [16]. The field E must satisfy Poisson equation. Using eqs (10) and (11) this gives

$$\varepsilon\frac{dE}{dx} = e\left(N_D + \frac{|J|}{ev_{pl}} + \frac{|J|}{e\mu_p^o E}\right) \tag{12}$$

where ε is the dielectric constant of the semiconductor.

Integrating eq. (12) gives the following equations [17]

$$W-S = \left[\frac{E}{\beta} - \frac{\alpha}{\beta 2}\ln(\alpha+\beta E)\right]_{E_S}^{E_W} \tag{13a}$$

$$V_S = \frac{1}{\beta^3}\left[\frac{(\alpha+\beta E)^2}{2} - 2\alpha(\alpha+\beta E) + \alpha^2\ln(\alpha+\beta E)\right]_{E_S}^{E_W} \tag{13b}$$

where E_S and E_W are the electric fields at x=S and x=W, and

$$\alpha = \frac{|J|}{\varepsilon \mu_p^0} \qquad \beta = \frac{e}{\varepsilon}\left(N_D + \frac{J}{e v_{pl}}\right) \tag{14}$$

E_S is derived from eqs. (10) and (6b). Thus eqs. (13ab) define V_S as a function of W-S and J.

A similar approach is used for the calculation of V_{S^*}.

2.4 General Strategy

We have to solve the plasma equations, i.e. eq.(3) with boundary conditions given by eqs. (5ab) to (8ab), subject also to the circuit conditions given by equation (1), where V_{DIODE} (t) depends on J, S and S^*, that is on the solution found in the plasma.

The solution proceeds by time steps δt. The strategy for the calculation is given in the schematic flow diagram shown in Fig. 3.

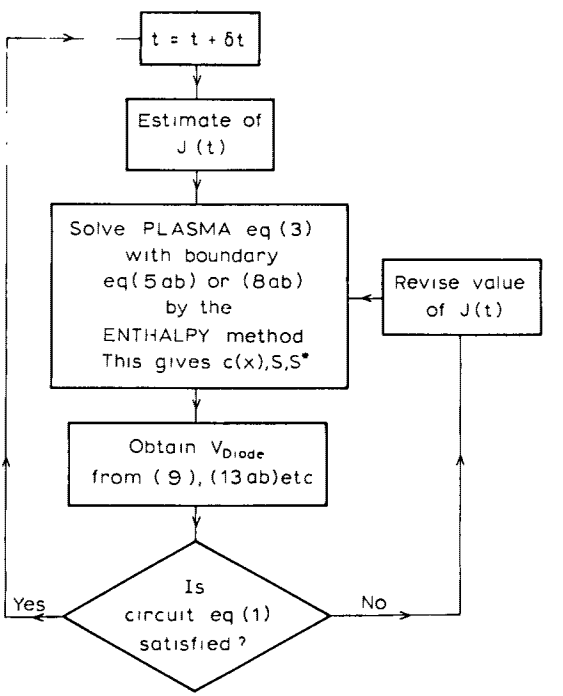

Fig 3.

As shown in this diagram the plasma equations are solved by means of the Enthalpy Method. The latter will be described in the next subsection.

2.5 The Enthalpy Method

The Enthalpy Method gets its name from its first use for heat problems (see section 1). The enthalpy of a substance is by definition its heat content per unit volume. Thus the enthalpy H_l of a liquid at temperature T is related to the enthalpy H_s of a solid at the melting temperature T_f by the equation

$$H_l = H_S + \rho_l c_l (T-T_f) + L \tag{15}$$

where ρ_l is the density of the liquid, c_l is its specific heat, and L the latent heat of fusion.

Eqs. (3) and (8ab) are very similar to those governing the solidification of a liquid contained between two parallel solid slabs, with a given rate of heat loss at the liquid/solid interfaces. Details of this similarity are given in [11], where the Enthalpy Method is used to calculate the decay of the plasma in a pin diode, for a given and constant reverse current.

We shall give again a description of the method, which we apply to the present problem. One has to solve at time t eq. (3) with boundary conditions given by eqs. (5ab) or (8ab), when knowing the solution at $t-\delta t$, and taking J(t) also as known (Fig. 3). The modelling of Phase 1 is fairly standard. The main difficulty lies in Phases 2 and 3 where the moving boundaries at $x=S(t)$ and $x=S^*(t)$ are not given.

The Enthalpy Method has the advantage over other methods [2,3] that during all phases of recovery it solves differential equations of the type given by eq. (3) over the whole range $0 < x < W$, at all phases instead of solving it only over the plasma, and the positions S(t) and $S^*(t)$ come out from the solution.

This is done by the following steps (see Fig. 4).

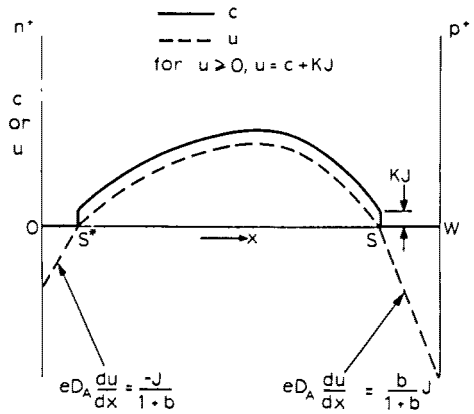

Fig 4

a) One defines c(x) over the range $0<x<W$ even in Phases 2 and 3, by assuming that c(x) falls abruptly from $K|J|$ to zero at the plasma boundaries and that

$$c(x) = 0 \text{ (outside of plasma)} \tag{16}$$

b) One introduces a continuous function u(x)

$$u(x) = c(x)+K|J| \text{ (in the plasma)} \tag{17a}$$

$$u = 0 \quad \text{at } x = S \text{ and } x = S^* \tag{17b}$$

with

$$\frac{\partial}{\partial x}\left[D_A \frac{\partial u}{\partial x}\right] = 0 \quad \text{(outside the plasma)} \tag{17c}$$

i.e. $D_A \partial u/\partial x$ remains constant over $0 \leq x < S^*$, and $S < x \leq W$.

With these definitions of c and u, equation (3) can be replaced by

$$\frac{\partial c}{\partial t} = \frac{\partial}{\partial x}\left[D_A \frac{\partial u}{\partial x}\right] - \frac{\sigma c}{\tau} \tag{18}$$

where $\sigma = 1$ for $c \geq K|J|$ and $\sigma = 0$ for $c < K|J|$.

Equation (18) is applied over the whole range. $0 \leq x \leq W$.

One adds the boundary conditions

$$e\, D_A \left.\frac{\partial u}{\partial x}\right|_0 = -\frac{J}{1+b} + eh_n\, c^2(o,t) + es_n\, c(o,t) \qquad (19a)$$

$$e\, D_A \left.\frac{\partial u}{\partial x}\right|_W = \frac{b}{1+b}\, J - eh_p\, c^2(W,t) - es_p\, c(W,t) \qquad (19b)$$

It can be checked that the solution of equation (18) over the whole base satisfies equations (5ab) or (8ab) at the plasma boundaries, due to the abrupt change of $c(x)$ at these boundaries and the selected values of $e\, D_A\, \partial u/\partial x$ outside the plasma (equation (19ab)) - see [11].

2.6 Numerical Solution

Using finite differences for equidistant mesh points in space, and a fully implicit formulation in time, one gets from equation (18)

$$c_n^i - c_n^{i-1} = \frac{\delta t}{\delta x^2}\left[D^i_{n+\frac{1}{2}}\left(u^i_{n+1} - u^i_n\right) - D^i_{n-\frac{1}{2}}\left(u^i_n - u^i_{n-1}\right)\right] - \delta t \sigma^i_n\, c^i_n/\tau \qquad (20)$$

δx is the mesh spacing. The index n stands for the mesh point at $x_n = n\,\delta x$. $D_{n\pm\frac{1}{2}}$ stands for the average values of D_A between the points x_n and x_{n+1}. The index i stands for the time t_i at which a solution is sought, and the index i-1 corresponds to the time $t_{i-1} = t_i - \delta t$, for which a solution has already been obtained.

At the base boundaries n = 0 (x = 0) and $n = n_w$ (x = W) one uses also equation (20), from which u_{-1} and u_{n_w+1} are eliminated by means of equation (19ab) which take the form

$$e\, D_o \frac{u_1 - u_{-1}}{2\delta x} = -\frac{J}{1+b} + eh_n\, c_o^2 + es_n\, c_o \qquad (21a)$$

$$e\, D_{n_w} \frac{u_{n_w+1} - u_{n_w-1}}{2\delta x} = \frac{b}{1+b}\, J - eh_p\, c_w^2 - es_p\, c_w \qquad (21b)$$

Equation (20) is then solved using the Gauss Seidel iteration procedure. One gets at the k-th iteration

$$c^{i,k}_n + \frac{\partial t}{\partial x^2}\left[D^{i,k-1}_{n+\frac{1}{2}} + D^{i,k-1}_{n-\frac{1}{2}}\right] u^{i,k}_n = G^{i,k}_n \qquad (22)$$

where $G^{i,k}_n$ is obtained from the (k-1)th iteration

$$G^{i,k}_n = \frac{\delta t}{\delta x^2}\left[D^{i,k-1}_{n+\frac{1}{2}}\, u^{i,k-1}_{n+1} + D^{i,k-1}_{n-\frac{1}{2}} u^{i,k}_{n-1}\right] - \delta t\, \sigma^{i,k-1}_n c^{i,k-1}_n / \tau + c^{i-1}_n \qquad (23)$$

Using equations (17ab) and Fig. 4, one can put the l.h.s. of equation (22) in terms of $c^{i,k}_n$ or $u^{i,k}_n$ alone in three distinct forms, corresponding to 3 ranges in the value of $G^{i,k}_n$.

a) If $G^{i,k}_n < 0$ equation (22) gives

$$c^{i,k}_n = 0, \quad \frac{\delta t}{\delta x^2}\left(D^{i,k-1}_{n+\frac{1}{2}} + D^{i,k-1}_{n-\frac{1}{2}}\right) u^{i,k}_n = G^{i,k}_n \qquad (24a)$$

b) If $0 \leq G^{i,k}_n < -KJ$:

$$c^{i,k}_n = G^{i,k}_n \quad , \quad u^{i,k}_n = 0 \qquad (24b)$$

c) If $G^{i,k}_n \geq -KJ$:

$$\left[1 + \frac{\delta t}{\delta x^2}\left(D^{i,k-1}_{n+\frac{1}{2}} + D^{i,k-1}_{n-\frac{1}{2}}\right)\right] c^{i,k}_n = G^{i,k}_n - \frac{\delta t}{\delta x^2}\left(D^{i,k-1}_{n-\frac{1}{2}} + D^{i,k-1}_{n+\frac{1}{2}}\right) KJ$$

$$u^{i,k}_n = c^{i,k}_n + KJ \qquad (24c)$$

Equations (24abc) give the values of $c^{i,k}_n$ and $u^{i,k}_n$ and the problem is therefore solved.

S and S^* are the abscissae where u = 0 (see eq. (17b) and Fig. 4). They do not usually fall on mesh points, but are obtained by linear extrapolation from the range where $u<0$.

2.7 Examples of Results

As an illustration of the Enthalpy method, results will be given here showing the effect of the circuit on a diode whose characteristic parameters are given in Table I below:

Table I Diode Parameters

$W = 100\ \mu m$	Cross sectional area $= 0.1\ cm^2$
$N_d = 2 \times 10^{14}\ cm^{-3}$	$\tau = 0.9\ \mu s$
$h_n = h_p = 2 \times 10^{-14}\ cm^4\ s^{-1}$	$s_n = s_p = 3000\ cm\ s^{-1}$

Figs. 5 to 7, as well as Fig. 2ab refer to this diode.

The forward current I_F was taken equal to 2 A and 20 A, V_R varied between 20 V and a few hundred volts, $|dI/dt|$ was taken as 20 A/μs, 50 A/μs and 100 A/μs. The computation of each recovery took 1 to 10 mins on the IBM 4381 computer.

Fig. 5 shows recovery for fairly standard test conditions. Also shown in this figure are the definitions of I_{RR}, t_o and t_{rr}.

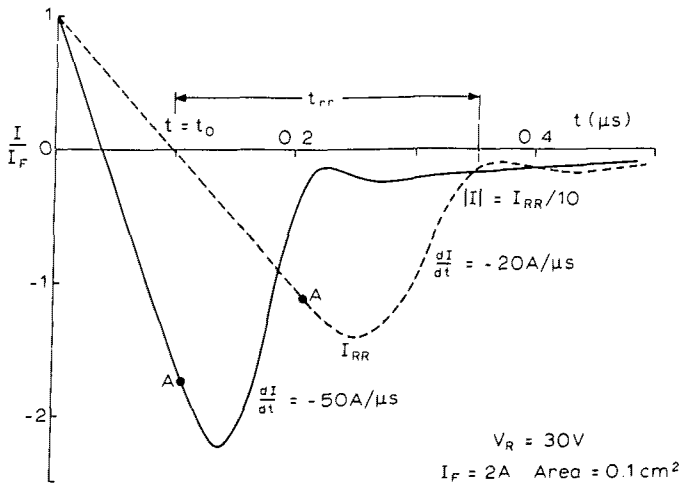

A● Corresponds to point where plasma detaches itself from p⁺ı junction

Fig 5.

Fig 6 gives the variations in recovery current for a larger value of I_F (I_F = 20 A) and various values of dI/dt and of V_R (V_R < 200 V). Modelling at V_R > 300 V showed avalanching occurring slightly beyond I_{RR}.

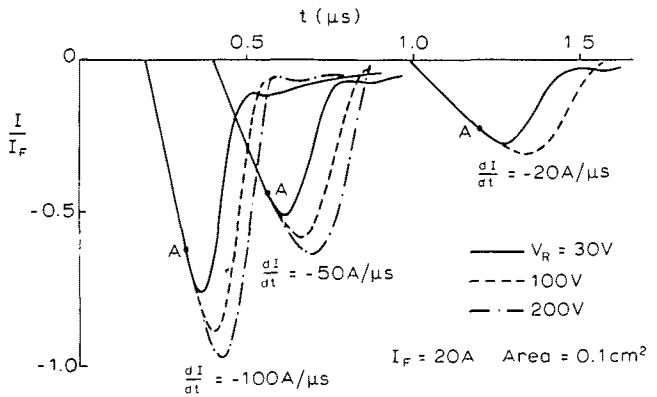

Fig 6.

It is seen in Figs 5 and 6 that the point A, where the plasma detaches itself from the base/p^+ junction, corresponds to values of $|I|$ which are sometimes appreciably below I_{RR}.

Fig. 7 shows the charge recovered by the current between the times $t = t_o$ and $t = t_o + t_{rr}$ ($I(t_o) = 0$ $|I(t_o + t_{rr})| = I_{RR}/10$) for various values of the circuit parameters. This charge varies between 20% and 60% of the total charge held in the base under steady state.

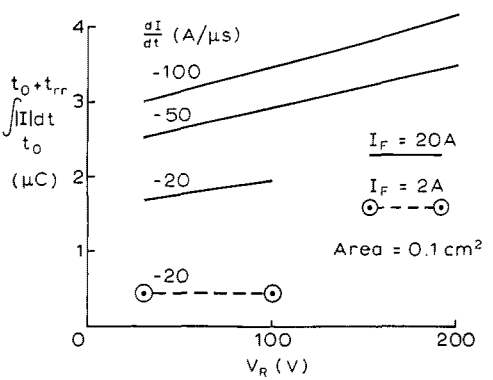

Fig.7.

Table II sums up the effect of I_F, $|dI/dt|$ and V_R on current recovery (e.g. figs. 5, 6, 7) and on V_{MAX} (one finds that $2.6 < V_{MAX}/V_R < 5$).

Table II Effect of Circuit on Ramp Recovery

	Increase in I_F	Increase in $\lvert dI/dt \rvert$	Increase in V_R
$\frac{I_{RR}}{I_F}$	Decreases (but I_{RR} increases)	Increases	Increases
Curve I(t) (for I<0)	Widens	Narrows	Widens
t_{rr}	Increases	Decreases	Decreases for $V_R < 100V$ Nearly constant for $V_R > 100V$
$Q_I = \int_{t_o}^{t_o+t_{rr}} I\, dt$	Increases (but Q_I/I_F decreases)	Increases	Increases
$\frac{V_{MAX}}{V_R}$	Small effect	Decreases	Small changes for $30V<V_R<100V$ Increases for $V_R > 100V$

It has to be noted that although an increase in V_R widens the I(t) curve, it does not increase t_{rr} for the diode described here (Table II). This is due to the fact that as V_R increases the drop of current with time becomes more abrupt in the last stages of recovery (see Fig. 6); for V_R small the final current decay is slow and exhibits some oscillations, such as could be found in an L-C circuit.

When modelling other diodes however we have found that an increase in V_R can produce an increase in t_{rr} and also an increase in the charge extracted by the current. With these exceptions most of the trends reported in Table II appear to be applicable to a wide range of diodes.

3. G.T.O. THYRISTOR TURN-OFF

We shall consider the computation of the characteristics of a GTO thyristor turn-off in the snubber circuit of Fig. (8), by the Enthalpy method. The structure of a GTO thyristor and the plasma decay in the wide lightly-doped n-base is illustrated in Fig. (9). The same general features of hole extraction at the (gate) blocking junction in the n-base occur as in the p-i-n diode. However during the switch off process, which is initiated by the switch in the gate circuit, hole injection continues at the anode junction while the carrier density falls at the gate junction with the eventual formation of a space charge layer. The electrons

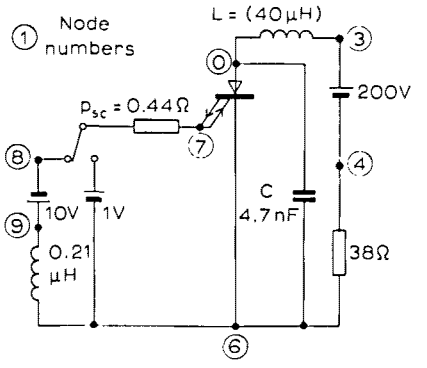

Fig 8

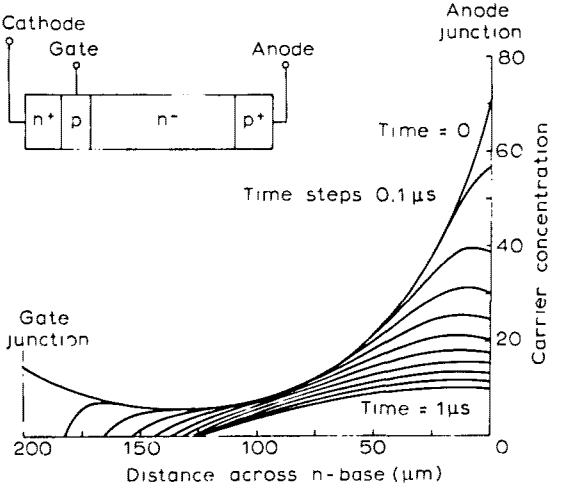

Fig. 9.

in the n-base can only disappear by recombination during this process. When the space charge layer is produced the anode current falls to a fraction of its ON state value. As in the p-i-n diode, the space charge layer subsequently expands causing the voltage across the device to rise. The electron-hole plasma which is trapped between the layer and the anode junction decays by recombination and the remaining anode current slowly decreases with a characteristic 'tail' (Fig.10).

The basic equations given in the preceding sections for the variation of the electron-hole plasma in the base of the

p-i-n diode can be applied directly to the situation in the lightly-doped base of the GTO thyristor. The only difference is the boundary condition for the carrier density gradient at the gate junction when the plasma touches the junction, which is (with $J>0$ and $J_K>0$)

$$e\, D_A \frac{\partial c}{\partial x}\bigg|_W = \frac{b}{1+b} J - \alpha_{n-p-n}.J_K \qquad (25)$$

where α_{n-p-n} is the transport factor of the p-base and J_K is the cathode current density. The plasma always touches the other junction so that eq. (5b) is always used at that boundary.

The Enthalpy method has been applied to the GTO thyristor calculation in a different form to that described previously, in that its equations are translated into a circuit form, and then solved, together with the equations for the circuit external to the device, by a circuit analysis program, PHILPAC [19]. This procedure has the advantage that changes to the external circuit can readily be taken into account, however it has a drawback that the details of the numerical procedures involved are not so directly under the control of the user.

4. CIRCUIT SOLUTION

The equation for the carrier density inside the plasma, eq. (3), has the same form as that for voltage on a transmission line composed of series resistance and shunt capacitance and conductance elements. The equation for this voltage is

$$\frac{\partial}{\partial x}\left[\frac{1}{R}\frac{\partial V}{\partial x}\right] = c\frac{\partial V}{\partial t} + GV \qquad (26)$$

where R, C and G are the series resistance, shunt capacitance and conductance per unit length respectively. By defining C and G to be non linear functions of V in the following way

$$C = \begin{cases} C' & V \geq 0 \\ 0 & V < 0 \end{cases}$$

$$G = \begin{cases} G' & V \geq 0 \\ 0 & V < 0 \end{cases} \qquad (27)$$

we can reproduce eqs. (16) to (18) with K=0. The boundary conditions of eqs. (19) can be obtained by terminating the transmission line by circuit components consisting of current generators and linear and square law resistors. A circuit analysis of the network represented by these equations enables the junction carrier densities and the width of the space charge layer (if present) to be computed in circuit terms and from this the voltage across the n-base can be obtained as a function of the anode current and time. Representing this voltage as a voltage generator it can be added to other circuit elements which model the remaining regions of the thyristor, i.e. the p base and the n^+ emitter, to form a complete model for the device [18]. The program, PHILPAC, used for such simulations has the advantage that it can handle the non linear functions of G and C in eq. (27) and in addition assign to voltage and current generators values derived from expressions containing voltages and currents in other parts of the cicuit.

5. COMPUTED RESULTS OF G.T.O. THYRISTOR TURN-OFF

The circuit solution of the 'Enthalpy method' equations applied to the GTO thyristor has been used to compute current and voltage waveforms in a GTO thyristor with a wide lightly-doped n-base switched off from an ON state anode current of 5 Amps in the snubber circuit of Fig. (8). The parameters of the thyristor were as follows

Area = 4 sq. mm., $\alpha_{n-p-n} = 0.80$, W_B(n-base) = 200 μm,

N_D(n-base) = $10^{14}cm^{-3}$, τ (n-base) = 1 μs,

At the anode junction $h_p = 2.10^{-14}cm^4/s$, $s_p = 0$ cms/s

with the circuit components having values

C_s = 4.7 nF, L_s = 40 μH, R_s = 38Ω, V_s = 200V, V_g = 10V,

L_g = 0.21 μH.

These circuit components giving an initial dV_{AK}/dt of 1 kV/μs during switch off, Fig. (10) shows the computed anode current and voltage waveforms together with experimental results. The power dissipated in the device during turn-off is an important quantity, and Fig. (10) also shows a plot of this. The total energy, E_T, dissipated in the thyristor during switch-off should be as small as possible. In Fig. (11) the variation of E_T with n-base lifetime, width, and doping density is shown for the circuit and device conditions given above. It can be seen from these results that the energy loss is reduced by decreasing the base lifetime, raising the base doping density, and increasing the base width.

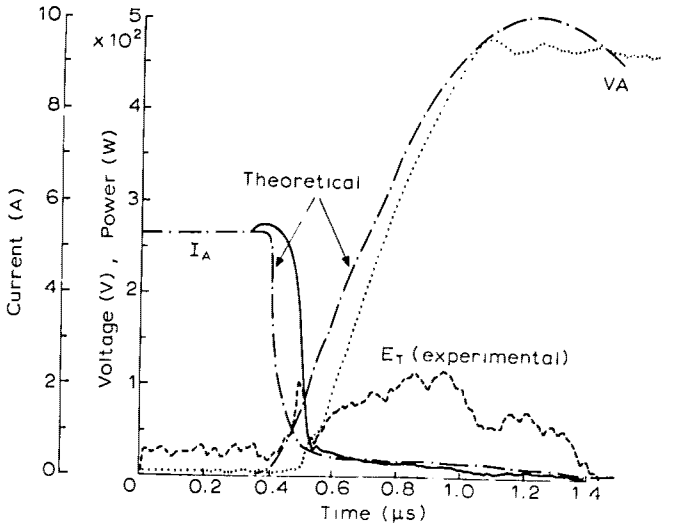
Current (A)
Voltage (V), Power (W)
x10²
Time (μs)
Theoretical
VA
I_A
E_T (experimental)

Fig 10

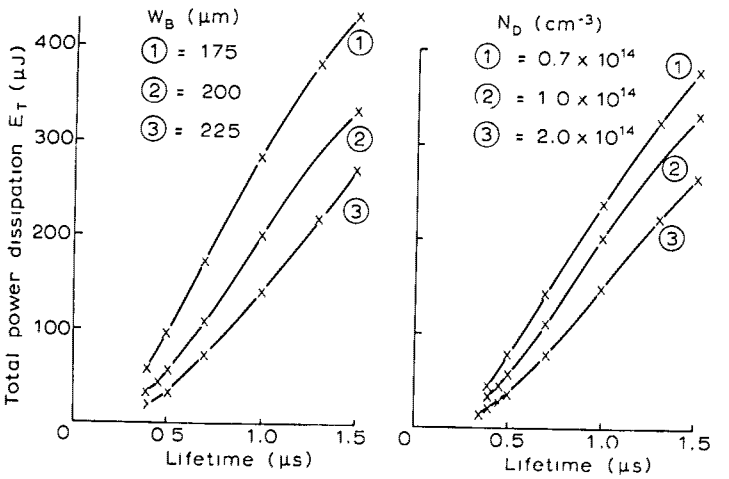
Total power dissipation E_T (μJ)
W_B (μm)
① = 175
② = 200
③ = 225
Lifetime (μs)
N_D (cm⁻³)
① = 0.7 x 10¹⁴
② = 1.0 x 10¹⁴
③ = 2.0 x 10¹⁴
Lifetime (μs)

Fig 11

It is possible to reverse the polarity of the layers of the n-base thyristor to produce a thyristor with a wide lightly doped p-base, see Fig. (12). The switch-off of this device in the reverse polarity version of the circuit of Fig. (8), with the same circuit and device constants as for the n-base device, is compared with the n-base result in Fig. (13), which shows the anode current variation with time. It can be seen that the p-base thyristor has a longer storage and fall time. It would be expected that this would cause a larger power dissipation in the p-base device and this is confirmed by the plots of Fig. (14). This work would suggest that there are disadvantages to the use of p-base GTO thyristors in switching circuits.

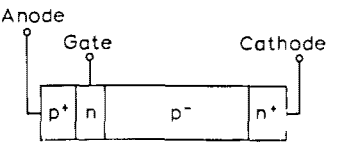

Fig 12

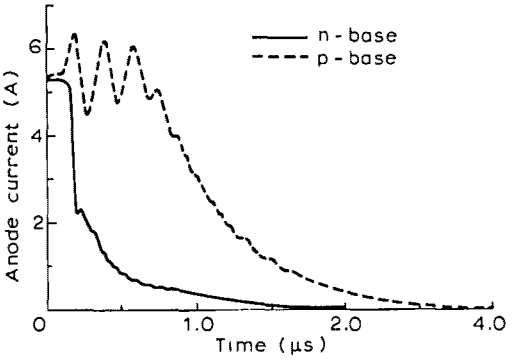

Fig. 13

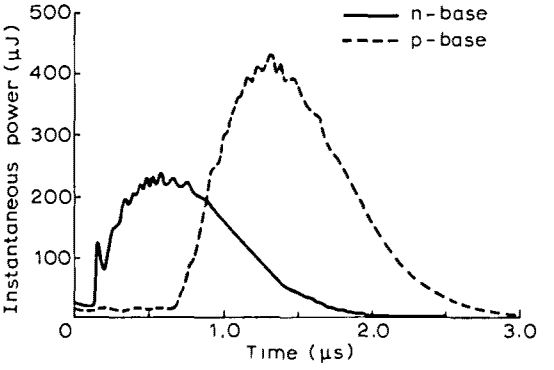

Fig. 14.

These results have been obtained with the use of a one-dimensional model. However the electron-hole plasma in the wide lightly doped base of the thyristors is also compressed in directions parallel to the junctions as well as in a normal direction during switch-off. For a full model of the devices this effect should be taken into account although, for the circuit conditions quoted, reasonable agreement has been obtained between the one-dimensional predictions and experiment.

6. CONCLUSIONS

The Enthalpy method provides a rapid way of computing the time dependent characteristics of a semiconductor device whose behaviour is critically determined by the movement of the boundaries of an electron-hole plasma in a base of the device.

7. ACKNOWLEDGEMENTS

The authors are grateful to Dr. J. Ockendon, Dr. A.B. Crowley and other members of the Mathematical Institute, Oxford, for introducing them to the 'Enthalpy' Method. The authors are also indebted to Mr J. Pritchard of Philips Research Laboratories, and Mr D. Gibbs of Philips ISA for assistance, and to Mr A. Davidson and Mr J. Piesing.

8. REFERENCES

[1] BENDA, H. and SPENKE, E., Proc. IEEE, 55, 1331 (1967).

[2] MUNOZ VAGUE, A., These de Doctorat d'Etat, Universite Paul-Sabatier, Toulouse, 1977.

[3] CHANTE, J.P., These de Doctorat d'Etat, Universite Claude Bernard, Lyon, 1981.

[4] BISIO, G.R. and PIDATELLO, S., Nasecode 1, Dublin 1979, p.188, Ed. B.T. Browne and J.J.H. Miller Boole Press, 1979).

[5] ELLIOTT, C.M. and OCKENDON, J.R., Weak and Variational Methods for Moving Boundary Problems, Pitman, 1982)

[6] CARSLAW, H.S. and JAEGER, J.C., Conduction of Heat in Solids, Oxford Clarendon Press, 1978.

[7] BERZ, F., Sol. State Electron. 23, 783 (1980).

[8] BIANCO, B., BISIO, G.R., DELFINO, R., IEEE Tr. ED-27, p.1834 (1980).

[9] SLATTER, J.A.G., WHELAN, J.P., Sol. State Electr. 23, 1235 (1980).

[10] COOPER, R.W., Sol. State Electr. 26, 217 (1983)

[11] BERZ, F., PRITCHARD, J. and CROWLEY, A.B., To be published in Sol. State Electron.

[12] KRAUSSE, J., Sol. State Electron. 15, 1377 (1972)

[13] BERZ, F. and SLATTER, J.A.G., Sol. State Electron. 25, 693 (1982).

[14] SCHLANGENOTTO, H. and MAEDER, H., IEEE, Trans. Elec. Dev., Ed-26 (3), 191 (1979).

[15] HERLET, A., Sol State Electron. 11, 717 (1968).

[16] CAUGHEY, D.N., THOMAS, R.E., Proc. IEEE, 55, 2191 (1967)

[17] BERZ, F., To be submitted to Sol. State Electr.

[18] GOUGH, P.A., To be submitted to IEEE Trans. Elec. Dev.

[19] PHILPAC - A Proprietary circuit analysis program developed by the Philips Co.